J. Phys. B: At. Mol. Opt. Phys. **33** (2000) 1211–1221. Printed in the UK PII: S0953-4075(00)08998-7

Ionization of hydrogenic targets by electron impact. Scaling laws

C R Stia, O A Fojón and R D Rivarola

Instituto de Física Rosario, CONICET-UNR and Escuela de Ciencias Exactas y Naturales, Facultad de Ciencias Exactas, Ingeniería y Agrimensura, Av. Pellegrini 250, 2000 Rosario, Argentina

Received 26 October 1999, in final form 18 January 2000

Abstract. A simple scaling law is obtained for ionization of hydrogenic targets by impact of fast electrons. This law is shown to be exact for the first-order Born approximation when $M_T \gg 1$ (with M_T the target mass) independently of the kinematical conditions considered. For high enough target nuclear charges, the scaling is proven to be valid in a Coulomb–Born approximation (CBA) in which correct boundary conditions are included in the initial wavefunction. The scaling formula is also studied for an extension with correct initial boundary conditions of the model introduced by Brauner, Briggs and Klar (BBK) in which an approximation to the exact final wavefunction is made, taking into account properly the asymptotic Coulombic character of the interactions between the aggregates of the collision system. In this case, the validity of the scaling is shown for a coplanar asymmetric geometry. At high enough impact energies, the scaling law works well for smaller target nuclear charges when the CBA and the BBK theoretical descriptions are used.

1. Introduction

The ionization of atomic species by electron impact is one of the simplest reactions leading to three unbound charged particles in the final channel interacting through Coulomb potentials. This kind of reaction is of interest in many fields such as astrophysics, controlled nuclear fusion, short-wave laser development, plasma physics and medical physics. The theoretical description of this process is a difficult task because the motion of the three particles remains correlated even at infinite separations due to the long range of the Coulomb forces.

In the case of neutral hydrogen targets, a model (hereafter referred to as BBK (Brauner, Briggs and Klar)) has been developed taking into account the correct asymptotic behaviour of the three-body problem in the final channel of the reaction [1]. A similar model was first proposed to study ionization of hydrogen atoms by proton impact [2]. The BBK model shows a very good agreement with experimental data [3, 4] of triple differential cross sections (TDCS) in a coplanar asymmetric geometry in an energetic domain in which the first Born approximation (FBA) is not able to reproduce the experiments [1].

In particular, hydrogenic ions with their simple electronic structure are easy to handle theoretically and can bring a deeper understanding of ionization reactions of more complex targets. However, reactions with hydrogenic systems are not easily performed. Preparation and experimental control of the target require great effort and the related intensity problems make this kind of measurement extremely difficult. As a result, in most ionization experiments involving ionic targets only total and single differential cross sections have been measured

0953-4075/00/061211+11$30.00

[5–12]. In particular, measurements of the total ionization cross section from the ground state of He^+ have been performed [13, 14] as well as Li^{2+} [15]. Data concerning multiply charged ions up to Ar^{17+} were obtained by modelling the charge evolution of ions in a trap [16].

Only recently, advancements in experimental techniques combining heavy-ion storage rings with electron cooling devices have made it possible to perform more elaborate measurements in electron–ion collisions [17–19].

Experiments addressed to measured TDCS for photon-impact ionization are presently underway [20]. It is well known that TDCS give the most detailed information about the ionization reaction providing an excellent test to theoretical models. This fact adds interest to the computation of TDCS for electron-impact ionization serving as a guide to obtaining proper double, single and total cross sections and to motivate future experimental work.

In the ionization reaction of hydrogenic targets by electron impact, the aggregates of the collision interact asymptotically through Coulomb potentials. This complicates the theoretical treatment of ionization of H-like targets with respect to the case of neutral atoms due to the fact that the long-range electron–ionic target must be taken into account properly in the initial channel of the collision. At the same time, this difficulty adds interest to the subject because new physical effects may appear in the dynamics of the reaction. Recently, the influence of nuclear charges and the mechanism to produce forward peaks for (e, 2e) reactions of H-like ions were studied [21]. It has been shown that the forward peak disappears if the incident Coulomb wave describing the electron–ionic target interaction is replaced by an incident plane wave. These are only theoretical predictions but after the work of Marrs [17] and Moores and Reed [22] using the super-electron beam ion trap (super EBIT) there exists some indication that the corresponding experimental check is possible.

Some calculations have been done for ionization of hydrogenic targets but the final wavefunction employed in these works either does not satisfy the correct asymptotic three-body boundary conditions [23] or is suitable only for highly asymmetric collisions [24]. A generalization of the BBK approximation for hydrogenic targets has been developed [21, 25, 26] treating the asymptotic conditions in the entry and final channels of the reaction in the proper way. Triple differential cross sections of ionization for hydrogenic ions are computed in the intermediate- and high-energy regimes, for coplanar symmetric and for coplanar asymmetric geometry.

In this work, TDCS are evaluated by using the extended BBK, CBA and FBA approximations for several hydrogenic targets. In a previous work [27], a scaling formula has been obtained allowing comparison of BBK and FBA cross sections resulting from the impact on hydrogen targets of projectiles with different masses. In studying TDCS for hydrogenic targets within the frameworks of the distorted-wave Born model and a CBA approximation with effective charges [28], Spivack and co-workers [20] found interesting qualitative similarities in the cross sections for different target nuclear charges Z_T when the excess energy of the incident electron is scaled by Z_T^2 for a coplanar symmetric geometry. As a matter of fact, the shape of the cross sections turns out to be almost the same. And this is true not only in the case of the hydrogen isoelectronic sequence but also in the helium one. This striking feature is revisited here and further insight is gained by deriving a scaling law for the TDCS of different hydrogenic targets.

This paper is organized as follows. In section 2, the generalized BBK, CBA and FBA approximations are summarized. In section 3, the scaling law is obtained. In section 4, results and conclusions are given. Atomic units are used unless otherwise specified.

2. Theory

The reaction of interest is

$$e + (Z_T + e) \rightarrow e + Z_T + e \tag{1}$$

where Z_T is the nuclear charge of the target with mass M_T.

At the energies considered in this work, exchange and relativistic effects are negligible. The TDCS in the coplanar geometry is thus given by

$$\frac{d^3\sigma}{d\Omega_a\, d\Omega_b\, dE_b} = (2\pi)^4 \frac{k_a\, k_b}{K_i} |T_{if}|^2 \tag{2}$$

where $\boldsymbol{K}_i$, $\boldsymbol{k}_a$ and $\boldsymbol{k}_b$ are the momenta of the incident, the scattered and the ejected electrons, respectively, as measured from the centre-of-mass system. In the same expression, Ω_a and Ω_b are the solid angles subtended by the two outgoing electrons and E_b is the energy of the ejected electron.

For simplicity, the extended version of the BBK approximation is summarized in the following and the CBA and FBA approximations are obtained as particular cases.

The *prior* version of the transition matrix element reads

$$T_{if} = \langle \Psi_f^- | V_i | \Psi_i \rangle \tag{3}$$

where Ψ_i and Ψ_f^- are the initial wavefunction and the exact final wavefunction with correct incoming conditions, respectively, and V_i is the perturbation interaction in the initial channel.

The initial wavefunction Ψ_i is chosen as a product of a Coulomb wave and a bound wavefunction, i.e.

$$\Psi_i(\boldsymbol{r}_a, \boldsymbol{r}_b) = F_c(\boldsymbol{K}_i, \boldsymbol{r}_a)\, \varphi(\boldsymbol{r}_b) \tag{4}$$

with $\boldsymbol{r}_a$ and $\boldsymbol{r}_b$ the Jacobi coordinates which, to the order $1/M_T$, denote the projectile and the ejected electron position vectors, respectively, in a reference frame fixed to the target nucleus. Coordinates are sketched in figure 1.

The bound state wavefunction φ describing the electron in the initial ground state of the hydrogenic atom is given by

$$\varphi(\boldsymbol{r}) = (Z_T^3/\pi)^{1/2} \exp(-Z_T r). \tag{5}$$

The incident electron is represented by the Coulomb wavefunction $F_c(\boldsymbol{K}_i, \boldsymbol{r}_a)$ that is taken to be

$$F_c(\boldsymbol{K}_i, \boldsymbol{r}_a) = (2\pi)^{-3/2} \exp(-\pi\alpha_i/2)\, \Gamma(1 + i\alpha_i) \exp(i\boldsymbol{K}_i \cdot \boldsymbol{r}_a) \times {}_1F_1(-i\alpha_i; 1; i(K_i r_a - \boldsymbol{K}_i \cdot \boldsymbol{r}_a)) \tag{6}$$

where $\alpha_i = -(Z_T - 1)/K_i$. This wavefunction takes into account the long-range behaviour of the Coulomb interaction between the incident electron and the charged hydrogenic atom.

The projectile–target interaction V_i is thus given by

$$V_i = \frac{1}{r_{ab}} - \frac{1}{r_a} \tag{7}$$

with $\boldsymbol{r}_{ab} = \boldsymbol{r}_a - \boldsymbol{r}_b$. It is easy to show that this interaction vanishes asymptotically faster than a Coulomb potential (i.e. as $\boldsymbol{r}_a$ tends to infinity while $\boldsymbol{r}_b$ remains finite).

The final-state wavefunction Ψ_f^- is approximated as in the BBK model, i.e.

$$\Psi_f^- \simeq (2\pi)^{-3} \exp(i\boldsymbol{k}_a \cdot \boldsymbol{r}_a + i\boldsymbol{k}_b \cdot \boldsymbol{r}_b) C(\alpha_{PT}, \boldsymbol{k}_a, \boldsymbol{r}_a)\, C(\alpha_{eT}, \boldsymbol{k}_b, \boldsymbol{r}_b)\, C(\alpha_{eP}, \boldsymbol{k}_{ab}, \boldsymbol{r}_{ab}) \tag{8}$$

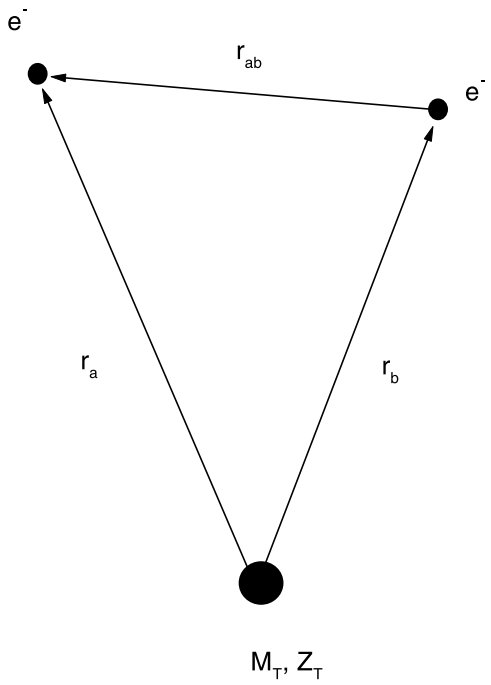

Figure 1. Coordinates used in the text.

where the Coulomb factors $C(\alpha, \boldsymbol{k}, \boldsymbol{r})$ are given by

$$C(\alpha, \boldsymbol{k}, \boldsymbol{r}) = \Gamma(1 - \mathrm{i}\alpha) \exp(-\pi\alpha/2)\, {}_1F_1(\mathrm{i}\alpha; 1; -\mathrm{i}(kr + \boldsymbol{k} \cdot \boldsymbol{r})) \tag{9}$$

and the Sommerfeld parameters α_{PT}, α_{eT} and α_{eP} are defined as

$$\begin{aligned} \alpha_{\mathrm{PT}} &= -Z_{\mathrm{T}}/k_a \\ \alpha_{\mathrm{eT}} &= -Z_{\mathrm{T}}/k_b \\ \alpha_{\mathrm{eP}} &= \frac{1}{2k_{ab}} \end{aligned} \tag{10}$$

with $\boldsymbol{k}_{ab} = \boldsymbol{k}_a - \boldsymbol{k}_b$, the momentum conjugate to $\boldsymbol{r}_{ab}$.

Finally, the T-matrix element may be written as

$$\begin{aligned} T_{if} = (2\pi)^{-9/2} N \left(\frac{Z_{\mathrm{T}}^3}{\pi}\right)^{1/2} \int \mathrm{d}\boldsymbol{r}_a\, \mathrm{d}\boldsymbol{r}_b \exp(\mathrm{i}\boldsymbol{K}_i \cdot \boldsymbol{r}_a - \mathrm{i}\boldsymbol{k}_b \cdot \boldsymbol{r}_b - \mathrm{i}\boldsymbol{k}_a \cdot \boldsymbol{r}_a) \\ \times {}_1F_1(-\mathrm{i}\alpha_i; 1; \mathrm{i}(K_i r_a - \boldsymbol{K}_i \cdot \boldsymbol{r}_a))\ {}_1F_1(-\mathrm{i}\alpha_{\mathrm{eT}}; 1; \mathrm{i}(k_b r_b + \boldsymbol{k}_b \cdot \boldsymbol{r}_b)) \\ \times {}_1F_1(-\mathrm{i}\alpha_{\mathrm{eP}}; 1; \mathrm{i}(k_{ab} r_{ab} + \boldsymbol{k}_{ab} \cdot \boldsymbol{r}_{ab}))\ {}_1F_1(-\mathrm{i}\alpha_{\mathrm{PT}}; 1; \mathrm{i}(k_a r_a + \boldsymbol{k}_a \cdot \boldsymbol{r}_a)) \\ \times \left(\frac{1}{r_{ab}} - \frac{1}{r_a}\right) \exp(-Z_{\mathrm{T}} r_b) \end{aligned} \tag{11}$$

where

$$N = \Gamma(1 + \mathrm{i}\alpha_{\mathrm{eT}})\, \Gamma(1 + \mathrm{i}\alpha_{\mathrm{eP}})\, \Gamma(1 + \mathrm{i}\alpha_{\mathrm{PT}})\, \Gamma(1 + \mathrm{i}\alpha_i) \exp\left(-\pi/2\, (\alpha_{\mathrm{eT}} + \alpha_{\mathrm{eP}} + \alpha_{\mathrm{PT}} + \alpha_i)\right). \tag{12}$$

The CBA matrix element may be obtained from equation (11) by taking the Sommerfeld parameters α_{PT} and α_{eP} equal to zero. In a similar way, the FBA matrix element is obtained by taking additionally $\alpha_i = 0$ and replacing the perturbation term $-1/r_a$ by $-Z_{\mathrm{T}}/r_a$. To the order $(1/M_{\mathrm{T}})$, these terms do not collaborate in the computation of T_{if} in the CBA and FBA models due to the orthogonality of the $(e-T)$ bound and continuum wavefunctions.

3. Scaling laws

In the following, a scaling law for the TDCS is derived. This scaling law is valid for asymmetric collisions when the incident energy and the nuclear charge of the target are sufficiently high.

Let us consider the following scaling in the incident energy:

$$E_i^{(Z_{\mathrm{T2}})} = \left(\frac{Z_{\mathrm{T2}}}{Z_{\mathrm{T1}}}\right)^2 E_i^{(Z_{\mathrm{T1}})} \tag{13}$$

which is equivalent to the following scaling in momenta:

$$\boldsymbol{K}_i^{(Z_{\mathrm{T2}})} = \left(\frac{Z_{\mathrm{T2}}}{Z_{\mathrm{T1}}}\right) \boldsymbol{K}_i^{(Z_{\mathrm{T1}})}. \tag{14}$$

The upper indices indicate that the magnitudes involved are those corresponding to the impact of an electron on a target of nuclear charge Z_{T}. From the energy conservation law (considering $M_{\mathrm{T}} \gg 1$),

$$\tfrac{1}{2}K_i^2 - \tfrac{1}{2}Z_{\mathrm{T}}^2 = \tfrac{1}{2}k_a^2 + \tfrac{1}{2}k_b^2 \tag{15}$$

it can be seen that the momenta $\boldsymbol{k}_a$ and $\boldsymbol{k}_b$ scale in the same way as $\boldsymbol{K}_i$ and consequently, the energies of the dispersed and ejected electrons, E_a and E_b, respectively, also scale in the same way. In the last formula, use has been made of the binding energy $\epsilon_i = -Z_{\mathrm{T}}^2/2$ of the ground state of a hydrogenic atom.

The Sommerfeld parameters α_{PT} and α_{eT} are invariant with respect to the scaling in momenta, i.e.

$$\alpha_j^{(Z_{\mathrm{T2}})} = \alpha_j^{(Z_{\mathrm{T1}})} \tag{16}$$

where j stands for PT and eT. In contrast, the Sommerfeld parameters α_{eP} and α_i do not behave in this way. As a matter of fact, applying the scaling to the α_i parameter one obtains

$$\alpha_i^{(Z_{\mathrm{T2}})} = -\frac{Z_{\mathrm{T2}} - 1}{Z_{\mathrm{T2}}} \frac{Z_{\mathrm{T1}}}{K_i^{(Z_{\mathrm{T1}})}}. \tag{17}$$

However, at a fixed incident energy $E_i^{(Z_{\mathrm{T}})}$ the scaling of α_i improves as Z_{T} increases. In this case,

$$\alpha_i^{(Z_{\mathrm{T2}})} \simeq -\frac{Z_{\mathrm{T1}}}{K_i^{(Z_{\mathrm{T1}})}} \simeq \alpha_i^{(Z_{\mathrm{T1}})}. \tag{18}$$

Now, the scaling applied to α_{eP} gives

$$\alpha_{\mathrm{eP}}^{(Z_{\mathrm{T2}})} = \frac{1}{Z_{\mathrm{T2}}} \frac{Z_{\mathrm{T1}}}{2k_{ab}^{(Z_{\mathrm{T1}})}} \tag{19}$$

and it can be seen that this parameter does not scale. However, if $k_{ab} \gg 1$ (coplanar asymmetric geometry), α_{eP} vanishes and consequently the corresponding hypergeometric function tends

to unity. This behaviour is also valid for the hypergeometric function in the entrance channel at high enough momentum $\boldsymbol{K}_i$ independently of the target nuclear charge.

In summary, at sufficiently high nuclear target charges and incident energies, wavefunctions and confluent hypergeometric functions scale or approximately scale. A similar analysis leads to the same conclusions with respect to the normalization constants of the Coulomb wavefunctions.

Let us now consider the following scaling for the independent coordinates:

$$\boldsymbol{r}_i^{(Z_{T2})} = \left(\frac{Z_{T1}}{Z_{T2}}\right) \boldsymbol{r}_i^{(Z_{T1})} \tag{20}$$

where $i = a, b$. According to this, the Jacobian transforms as

$$\mathrm{d}\boldsymbol{r}_a^{(Z_{T2})}\,\mathrm{d}\boldsymbol{r}_b^{(Z_{T2})} = \left(\frac{Z_{T1}}{Z_{T2}}\right)^6 \mathrm{d}\boldsymbol{r}_a^{(Z_{T1})}\,\mathrm{d}\boldsymbol{r}_b^{(Z_{T1})}. \tag{21}$$

Moreover, the coordinate $\boldsymbol{r}_{ab}$ transforms in the same way as $\boldsymbol{r}_{a,b}$.

Then, the T_{if} matrix element scales as

$$T_{if}^{(Z_{T2})}\left(E_i^{(Z_{T2})}, E_b^{(Z_{T2})}\right) = \left(\frac{Z_{T1}}{Z_{T2}}\right)^{7/2} T_{if}^{(Z_{T1})}\left(\left(\frac{Z_{T1}}{Z_{T2}}\right)^2 E_i^{(Z_{T2})}, \left(\frac{Z_{T1}}{Z_{T2}}\right)^2 E_b^{(Z_{T2})}\right). \tag{22}$$

Finally, the TDCS scales as

$$\frac{\mathrm{d}^3\sigma}{\mathrm{d}\Omega_a\,\mathrm{d}\Omega_b\,\mathrm{d}E_b}\left(Z_{T2}, E_i^{(Z_{T2})}, E_b^{(Z_{T2})}\right) = \left(\frac{Z_{T1}}{Z_{T2}}\right)^6 \times \frac{\mathrm{d}^3\sigma}{\mathrm{d}\Omega_a\,\mathrm{d}\Omega_b\,\mathrm{d}E_b}\left(Z_{T1}, \left(\frac{Z_{T1}}{Z_{T2}}\right)^2 E_i^{(Z_{T2})}, \left(\frac{Z_{T1}}{Z_{T2}}\right)^2 E_b^{(Z_{T2})}\right). \tag{23}$$

Keeping in mind that the FBA and CBA approximations may be obtained from the BBK model by setting to zero the corresponding Sommerfeld parameters, it is easy to show that the scaling formula obtained for the BBK approximation is also valid for the two first approximations. As in the FBA $\alpha_{PT} = \alpha_{eP} = \alpha_i = 0$, the scaling law is exact independent of the kinematical and geometric conditions. In the CBA where $\alpha_{PT} = \alpha_{eP} = 0$, the scaling is valid at high nuclear targets charges and incident energies for both the coplanar symmetric and asymmetric geometry.

4. Results and conclusions

Scaled TDCS with respect to the case of He^+ for coplanar asymmetric collisions are presented in the figures. In obtaining the TDCS, a numerical technique similar to that used in previous works on positronium formation has been employed [29]. Moreover, in order to make the computations of TDCS easier in the case of the extended BBK model, the following approximation has been made. In the Coulomb wavefunction given by equation (6), α_i is taken to be equal to zero. At the impact energies considered in this work, TDCS are only slightly modified by this approximation as the influence of the long-range Coulomb interaction in the initial channel is most important at low incident energies [25]. In contrast, the inclusion of the projectile–electron interaction in the exit channel has been shown to contribute even at high impact energies and must be considered in the calculations [25].

In the figures, scaled TDCS for target nuclear charge $Z_T = 2, 3, 4, 5$ are introduced. TDCS for $Z_T = 20$ are also shown and may be considered as a limiting case corresponding

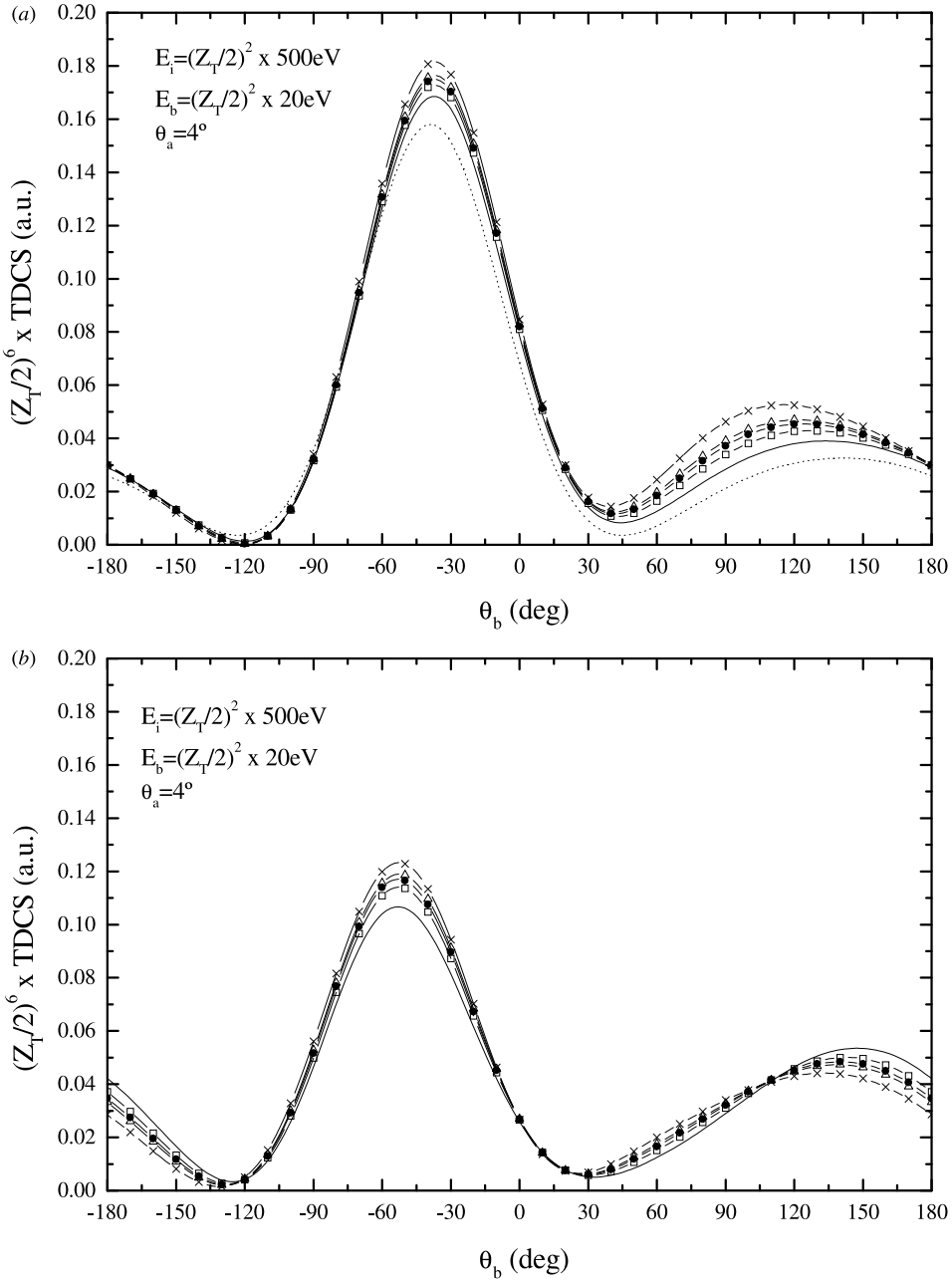

Figure 2. Scaled TDCS with respect to He^+ for electron-impact ionization for several hydrogenic targets, as a function of ejected angle θ_b. Incident energy $E_i = (Z_T/2)^2 \times 500$ eV. Ejection energy $E_b = (Z_T/2)^2 \times 20$ eV and scattering angle $\theta_a = 4^\circ$. The positive orientation for both angles is taken clockwise. (*a*) FBA and CBA results. ·····, FBA results. CBA results: He^+,——. Li^{2+}, —□—. Be^{3+}, —●—. B^{4+}, —△—. Ca^{19+}, —×—. (*b*) BBK results. Same notation as in (*a*).

to a high enough target nuclear charge. In figures 2(*a*) and (*b*), the scaled incident energy is $E_i = (Z_T/2)^2 \times 500$ eV, whereas in figures 3(*a*) and (*b*), $E_i = (Z_T/2)^2 \times 1$ keV and in figures 4

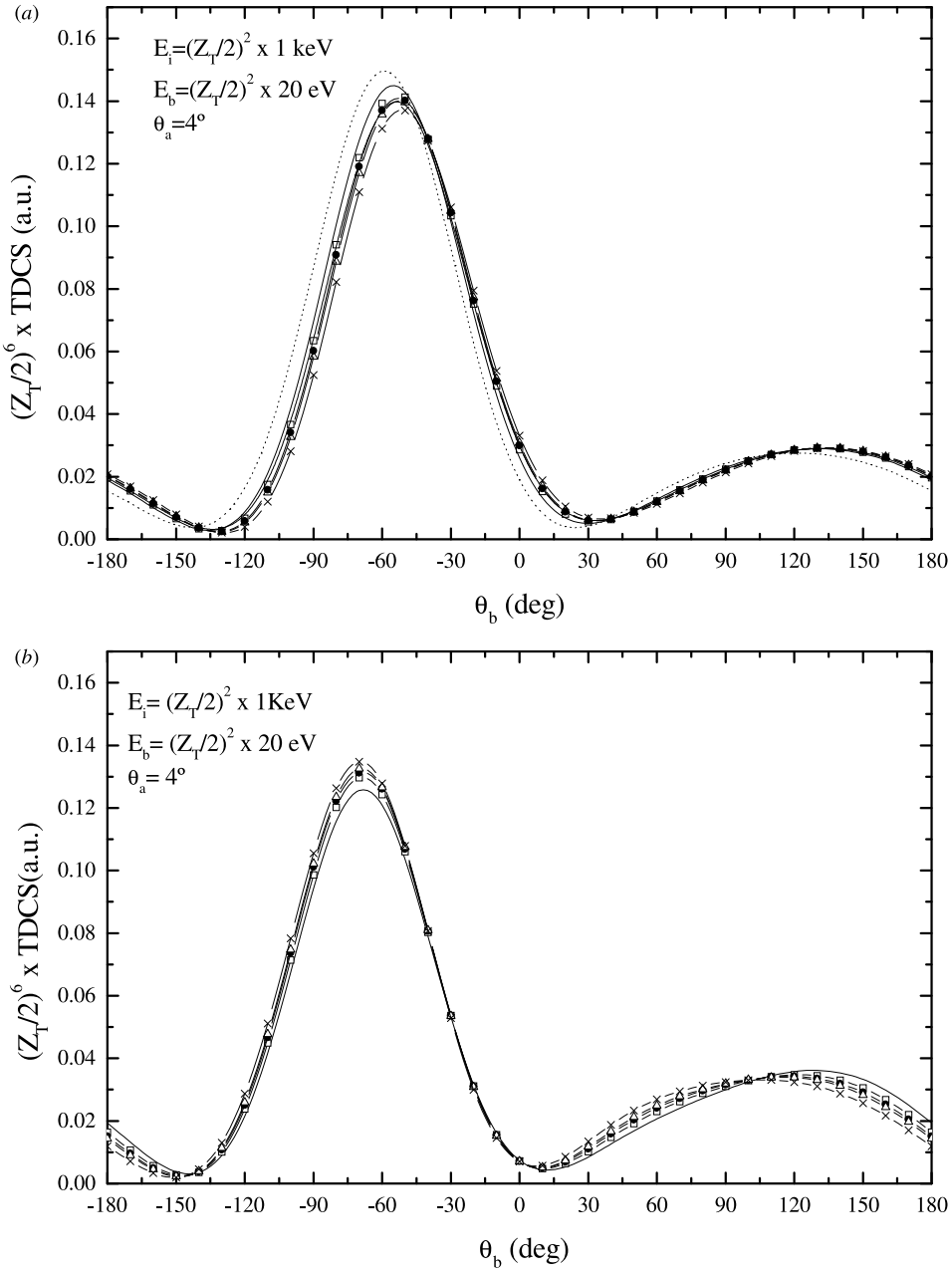

Figure 3. Same as in figure 2 but $E_i = (Z_T/2)^2 \times 1$ keV.

and 5, $E_i = (Z_T/2)^2 \times 4$ keV. In all the figures, the ejection energy is $E_b = (Z_T/2)^2 \times 20$ eV except in figure 5 where $E_i = (Z_T/2)^2 \times 80$ eV. FBA and CBA results are presented in figures 2(*a*) and 3(*a*) and extended BBK results are shown in figures 2(*b*), 3(*b*), 4 and 5. The last two figures are presented to analyse the behaviour of the BBK scaling at different asymmetric conditions. It can be seen that the scaling law works well in almost all the angular

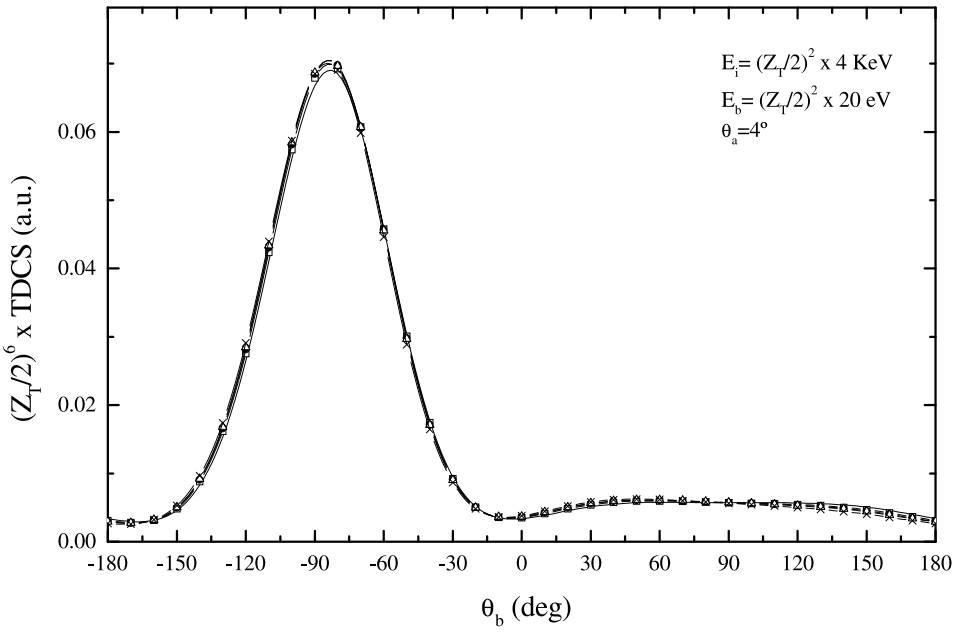

Figure 4. Same as in figure 3(*b*) but with an incident energy $E_i = (Z_T/2)^2 \times 4$ keV.

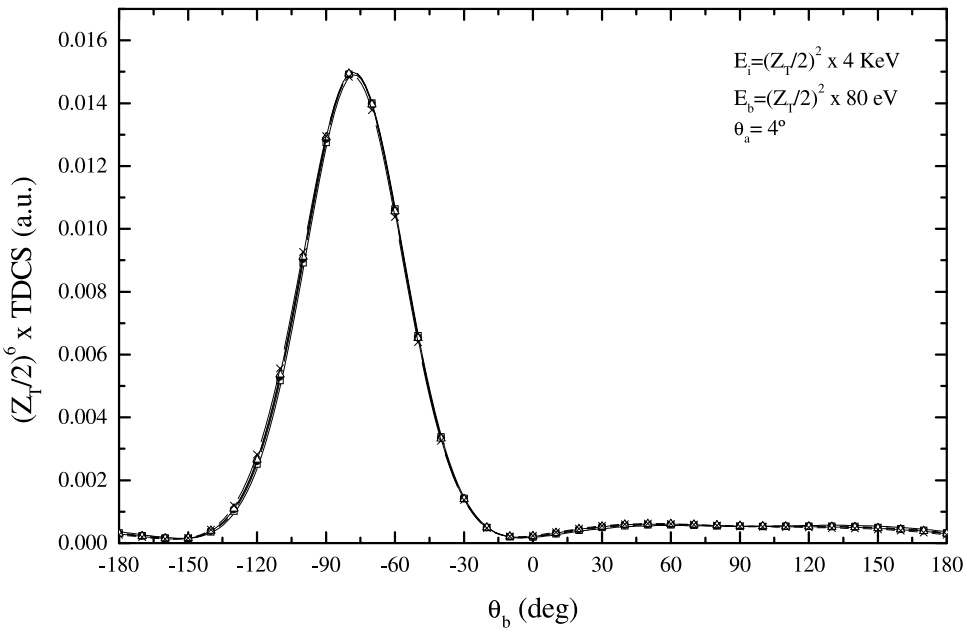

Figure 5. Same as figure 4 but with an ejection energy $E_b = (Z_T/2)^2 \times 80$ eV.

domain except in the angular region corresponding to the binary and recoil peaks where some discrepancies are found at the lowest incident energy considered. However, these deviations tend to disappear as the impact energy increases.

The differences found in scaled TDCS between CBA and FBA results for $E_i = (Z_T/2)^2 \times 500$ eV (see figure 2(*a*)) are a measure of the influence of the initial continuum wave factor. They increase in the binary encounter and recoil peaks as Z_T increases. Discrepancies remain between CBA and extended BBK approximations even at $E_i = (Z_T/2)^2 \times 1$ keV. For example, the maxima of the binary encounter peaks appear around $\theta_b \simeq 54^\circ$ in CBA and around $\theta_b \simeq 69^\circ$ in the extended BBK model.

To sum up, a scaling law for TDCS obtained within the generalized BBK, CBA and FBA approximations for hydrogenic targets have been presented. It is easy to show that the angular integrated cross sections verify a similar scaling law. The total cross section σ verifies the following scaling law:

$$\sigma\left(Z_{T2}, E_i^{(Z_{T2})}\right) = \left(\frac{Z_{T1}}{Z_{T2}}\right)^4 \sigma\left(Z_{T1}, \left(\frac{Z_{T1}}{Z_{T2}}\right)^2 E_i^{(Z_{T2})}\right). \tag{24}$$

The additional scaling factor $(Z_{T2}/Z_{T1})^2$ comes from the integration over the ejection energy E_b. This formula is in agreement with the classical scaling law predicted by Thomson [30]. Tinschert and collaborators [15] have performed a scaling of the available experimental data of total cross sections for hydrogenic ions following the Thomson law. They found that as the scaled incident energy increases, the scaling becomes valid. For scaled incident energies greater than $(Z_T/2)^2 \times 500$ eV the scaling works quite well. This may give an idea of the validity range of the present scaling law for TDCS.

The scaling law provides a simple tool to compute cross sections for hydrogenic targets with $Z_T > 2$ from the corresponding cross sections of He^+. This may be useful in designing future experiments with hydrogenic ions or in saving computer time in non-relativistic calculations involving highly charged hydrogenic targets.

Acknowledgments

This work was partially supported by the Agencia Nacional de Promoción Científica y Tecnológica (BID 802/OC-AR PICT no 03-04262) and the Consejo Nacional de Investigaciones Científicas y Técnicas de la República.

References

[1] Brauner M, Briggs J S and Klar H 1989 *J. Phys. B: At. Mol. Opt. Phys.* **22** 2265
[2] Garibotti G and Miraglia J E 1980 *Phys. Rev.* A **21** 572
[3] Ehrhardt H, Knoth G, Schlemmer P and Jung K 1985 *Phys. Lett.* A **110** 92
[4] Ehrhardt H 1988 Private communication appearing in Brauner M, Briggs J S and Klar H 1989 *J. Phys. B: At. Mol. Opt. Phys.* **22** 2265
[5] Dolder K T and Peart B 1976 *Rep. Prog. Phys.* **39** 693
[6] Crandall D H, Phaneuf R A, Hasselquist B E and Gregory D C 1979 *J. Phys. B: At. Mol. Phys.* **12** L249
[7] Younger S M 1980 *Phys. Rev.* A **22** 111
[8] Younger S M 1982 *Phys. Rev.* A **26** 3177
[9] Müller A, Hofmann G, Weissbecker B, Stenke M, Tinschert K, Wagner M and Salzborn E 1989 *Phys. Rev. Lett.* **63** 758
[10] Badnell N R, Griffin D C and Pindzola M S 1991 *J. Phys. B: At. Mol. Opt. Phys.* **24** L275
[11] Rachafi S, Belić D S, Duponchelle M, Jureta J, Zambra M, Hui Z and Defrance P 1991 *J. Phys. B: At. Mol. Opt. Phys.* **24** 1037
[12] Fang D, Hu W, Tang J, Wang Y and Yang F 1993 *Phys. Rev.* A **47** 1861
[13] Peart B, Walton D S and Dolder K T 1969 *J. Phys. B: At. Mol. Phys.* **2** 1347
[14] Defrance P, Brouillard F, Claeys W and van Wassenhove G 1981 *J. Phys. B: At. Mol. Phys.* **14** 103

[15] Tinschert K, Müller A, Hofmann G, Huber K, Becker R, Gregory D C and Salzborn E 1989 *J. Phys. B: At. Mol. Opt. Phys.* **22** 531
[16] Donets E D and Ovsyannikov V P 1980 *Report* P7-80-404 Joint Institute for Nuclear Research, Dubna, USSR (translation ORNL-tr-4702, available from Technichal Information Center, PO Box 62, Oak Ridge, TN 37830, USA)
[17] Marrs R E 1995 *19th Int. Conf. on the Physics of Electronic and Atomic Collisions* (Woodbury, NY: American Institute of Physics) p 705
[18] Müller A 1995 *19th Int. Conf. on the Physics of Electronic and Atomic Collisions* (Woodbury, NY: American Institute of Physics) p 317
[19] Sokell E, Currell F J, Shimizu H and Ohtani S 1999 *Phys. Scr.* T **80** 289
[20] Rath Spivack O, Rasch J, Whelan C T, Allan R J and Walters H R J 1998 *J. Phys. B: At. Mol. Opt. Phys.* **31** 845
[21] Shi Q, Chen Z, Chen J and Xu K 1997 *J. Phys. B: At. Mol. Opt. Phys.* **30** 2859
[22] Moores D L and Reed K J 1995 *Phys. Rev.* A **51** R9
[23] Roy A, Roy K and Sil N C 1982 *J. Phys. B: At. Mol. Phys.* **15** 1289
[24] Biswas R and Sinha C 1994 *Phys. Rev.* A **50** 354
[25] Jia X, Shi Q, Chen Z, Chen J and Xu K 1997 *Phys. Rev.* A **55** 1971
[26] Biswas R and Sinha C 1997 *J. Phys. B: At. Mol. Opt. Phys.* **30** 1589
[27] Berakdar J, Briggs J S and Klar H 1993 *J. Phys. B: At. Mol. Opt. Phys.* **26** 285
[28] Botero J and Macek J H 1991 *J. Phys. B: At. Mol. Opt. Phys.* **24** L405
[29] Fojón O, Rivarola R D, Gayet R, Hanssen J and Hervieux P A 1997 *J. Phys. B: At. Mol. Opt. Phys.* **30** 2199
[30] Thomson J J 1912 *Phil. Mag.* **23** 449